ACOUSTICS 2012

Tracking biopsy needle using Kalman filter and RANSAC algorithm with 3D ultrasound

Y. Zhao, H. Liebgott and C. Cachard

Centre de recherche en applications et traitement de l'image pour la santé, 7 avenue Jean Capelle, Bat Blaise Pascal, 69621 Villeurbanne Cedex
yue.zhao@creatis.insa-lyon.fr

Abstract — Ultrasound navigation technology is used for medical examinations and minimally invasive surgeries. This paper presents an improved method for tracking micro tools as biopsy metallic needles insertion using 3D ultrasound. Previously, the RANSAC [1] algorithm has been implemented to detect the needle inserted in human tissue in a stationary situation. In this paper, the Kalman filter is added to increase the stability of the RANSAC algorithm and realize an application in a dynamic situation. The RANSAC algorithm is used to get the needle axis direction and the position of the needle tip. The speckle tracking method is used to estimate the inserting speed of the needle. The Kalman filter uses the results given by the two methods above as the measurement to make the estimation of the direction of the needle and the position of the needle tip. The simulated results show that in both stationary and dynamic situations, the proposed method gives a more stable and accurate result than the RANSAC algorithm.
Keywords: RANSAC, Kalman filter, 3D ultrasound, tracking, simulation

1 Introduction

Nowadays, minimally invasive surgery is developing, so the ultrasound navigation technology is widely used in surgical operations. In this kind of surgical operations, the surgeons usually use 1D ultrasound probes to get 2D ultrasound images. With the 1D linear ultrasound probe, it is difficult to find the acquisition plane that contains the micro tools like therapy needles. Most time, the surgeons can only see part of the needle. What's more, some tissues have linear structures which can make the navigation system confused of needle and tissue. Furthermore the ultrasound image is very noisy, this point makes it extremely difficult to distinguish the needle from the background. So the 3D ultrasound guided technology and the precise navigation technologies are intense fields of research.

In 2D ultrasound imaging, a method used for needle localization, which depends on snake model and partial differential equation is proposed by B. Dong et al [2]. In 3D environment, a database based technology is introduced by S. Khosravi et al [3]. In this method, 2D cameras are used to establish a database containing the fixed needle of different positions and orientations. In the acquisitions, the needle position was estimated by finding the best fitted model in the database. In the domain of computed tomgraphy, an image guidance system named Image-Guided Surgery Toolkit has also been developed by Z. Yaniv et al [4]. A method using passive markers to track the surgical tools is proposed by J. Stoll and P. Dupont [5], and these markers fit for both 2D and 3D ultrasound systems. In 3D ultrasound domain, the parallel integral projection transform method and the RANSAC algorithm have been implemented for dectecting the metallic needle by Barva et al and by Uhercik et al [6], [7]. The RANSAC algorithm has the capability to detect the position of the needle in real time implementation [8], but it needs improvement in stability in case of a dynamic situation.

In this paper, a method to estimate and detect the position of the needle in a time series of Ultrasound (US) 3D volumes is proposed. This work is based on RANSAC algorithm, developed by Uhercik et al [7], which has been improved for detecting the position of the needle inserted using a 3D US volume acquisition. This new method also uses the Kalman filter and speckle tracking algorithm to make a dynamical procedure of tracking. Our proposition is to realize the prediction and the trajectory of the needle inserted in human's liver.

This paper is organized like below: section 2 summarized the methods used: Kalman filter, RANSAC algorithm and speckle tracking method; section 3 gives the simulation results and their statistical characteristics; the conclusion is given out in section 4.

2 Methods

2.1 Kalman Filter

2.1.1 Equations of Kalman filter

Kalman filter is an optimal recursive data processing algorithm. It was first published in 1960 by Kalman [9]. The Kalman filter is a set of mathematical equations that provides an efficient computational method to estimate the state of a process, in a way that minimizes the mean of the squared error [10]. This filter can predict the future state of a system, so it is very useful for the prediction of the position of the needle. The five main equations of Kalman filter can be divided into two parts.

The time updates equation:

$$\hat{x}_k^- = A\hat{x}_{k-1} + Bu_{k-1} \tag{1}$$

$$P_k^- = AP_{k-1}A^T + Q \tag{2}$$

The measurement updates equations:

$$K_k = P_k^- H^T (HP_k^- H^T + R)^{-1} \tag{3}$$

$$\hat{x}_k = \hat{x}_k^- + K_k(z_k - H\hat{x}_k^-) \tag{4}$$

$$P_k = (I - K_k H)P_k^- \tag{5}$$

Here, $\hat{x}_k^-$ represents the priori state estimate and $\hat{x}_k$ is the posteriori state estimate at step k ; A is the state transition matrix; B and u are the control matrix and control vector respectively; P_k^- is the priori estimate error covariance, and P_k is the posteriori estimate covariance at step k . R and Q are the measurement error covariance and processing error covariance respectively. K_k is the Kalman gain.

What should be paid more attention here is the processing error covariance Q , which indicates whether the mathematical model is adapted to the real situation or not; the measurement error covariance R , which affects the Kalman gain K_k . The Kalman gain K_k can weigh the importance of the innovation $(z_k - H\hat{X}_k^-)$.

2.1.2 Mathematical model

The objective of our research is to find the position of the needle. To fix a line in 3D space, three parameters are needed. According to the RANSAC algorithm, the parameters chosen are two direction angle α , β (Figure 1)

and the tip position (needle end). First, for the prediction of the position of the needle, 2 points belonging to the axis

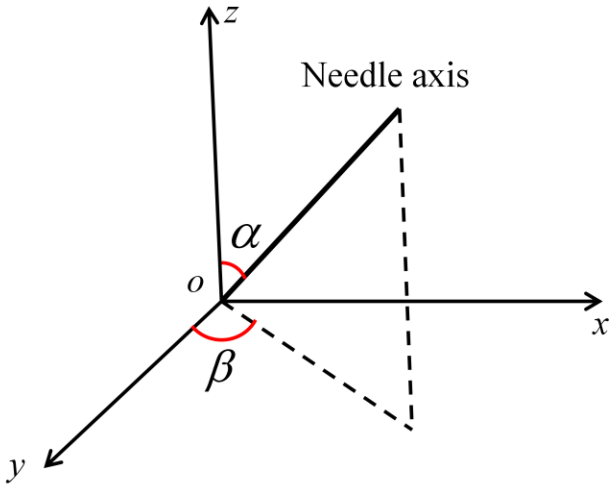

Figure 1: Positioning of the needle axis in the space (*o, x, y, z*)

of the needle can be obtained, so the unit direction vector of the tool's axis can be calculated. With the unit vector, the two direction angles can be obtained, and the needle axis is also fixed. Because different mediums have different echogenecities the ultrasound wave, the intensity of the metal needle along the axis is larger than that of the background. The tip position of the needle can be fixed where the intensity along the needle axis decreased drastically and does not increase anymore within a tolerence gap [6]. Supposing that in the insertion procedure, the needle only has a movement along the axis direction, and the inserting speed of the needle is changing from time to time. So the speed of needle tip should be included in the measurement vector. Assumming the needle is actuated by hand, the control input is unknown, so the control matrix B and the control vector u are set to zero. If case of a robotic driven needle insertion, there will be a control vector and control matrix as input. So the time update equations for the Kalman filter are

$$\hat{\mathbf{X}}_k^- = \mathbf{A}\hat{\mathbf{X}}_k \tag{6}$$

$$\mathbf{P}_k^- = \mathbf{A}\mathbf{P}_k\mathbf{A}^T + \mathbf{Q} \tag{7}$$

with $\mathbf{X} = [\alpha, \beta, \mathbf{p}_t, \mathbf{v}_t]^T$, $\mathbf{A} = \begin{bmatrix} \mathbf{I}_{2\times2} & \mathbf{0}_{2\times3} & \mathbf{0}_{2\times3} \\ \mathbf{0}_{3\times2} & \mathbf{I}_{3\times3} & \Delta t \times \mathbf{I}_{3\times3} \\ \mathbf{0}_{3\times2} & \mathbf{0}_{3\times3} & \mathbf{I}_{3\times3} \end{bmatrix}$,

Here notice that the position $\mathbf{p}_t$ and $\mathbf{v}_t$ are 3×1 vector, $\mathbf{p}_t = [x_t, y_t, z_t]$, $\mathbf{v}_t = [v_{tx}, v_{ty}, v_{tz}]$. The processing noise is a normal distribution which is the classic processing noise used in Kalman filters [9]. The measurement matrix is $\mathbf{H} = \mathbf{I}_{8\times8}$, so the measurement vector $\mathbf{Z} = \mathbf{X}$, and the measurement noise is also a normal distribution.

In the next two parts, the RANSAC algorithm used for measuring the position of the needle is first introduced, and then the speckle tracking method is used for measuring the speed of the needle.

2.2 RANSAC algorithm

The first objective is to get the position of the needle in a 3D ultrasound volume. Here the RANSAC algorithm is used to estimate the optimal axis for the position of the needle. Below are the four steps for RANSAC algorithm [7].

Step1: Thresholding — Reducing the number of voxels using the assumption that the intensity of the tool voxels is higher than the background.

Step2: Axis localization — Using RANSAC algorithm to estimate an approximate position of the needle axis. Here, we assume that the needle is a thin but straight line.

Step3: Local optimization — Finding a more accurate solution by using local optimization.

Step4: Tip localization — Identifying the endpoint of the tool along the tool axis.

2.3 Speckle tracking method

Speckle tracking method can directly track the backscattered echoes generated by ultrasonic scatters in tissue [11]. This method was first published by Robinson *et al*. [12], and then Trahey *et al*. [13]. It was first used to detect the blood velocity with ultrasound. Here speckle tracking method is used to measure the speed of the needle. This method can estimate velocities by estimating the displacement of a speckle pattern in the axial, lateral and elevation directions. First a small 3D region is chosen in the first volume as the kernel region, and this region is chosen according to the coordinate of the estimated tip position. Then a larger region is chosen as a searching region in the second volume, also this region is chosen around the known tip position. In the tracking procedure, the kernel region slides voxel by voxel in the searching region, and the normalized cross correlation (NCC) algorithm was chosen to compare the difference between the kernel region and the searching region. The 3D NCC is given in eq. (8). In the equation, ρ is the correlation coefficient, $\mathbf{X}_0$ is the kernel region, whose size is $m\times n\times p$, and $\mathbf{X}_1$ is the searching region. The size of ρ is related with the sizes of $\mathbf{X}_0$ and $\mathbf{X}_1$. Suppose $\mathbf{X}_1$ is size $M\times N\times P$, the size of ρ is $(M-m+1)\times(N-n+1)\times(P-p+1)$. However, the traditional NCC does not meet for the real time applications, so we choose the fast normalized cross correlation algorithm (FNCC) [14]. To calculate the numerator of eq. (8), the transform domain is used to improve the efficiency of calculation. Because the numerator part is like the form of convolution, and it is faster to compute the convolution in the frequency domain, so the fast Fourier transform (FFT) is used to transfer the numerator part to the 3D frequency domain, after the multiplication, the inverse FFT (IFFT) is

$$\rho(\alpha,\beta,\gamma) = \frac{\sum_{i=1}^{m}\sum_{j=1}^{n}\sum_{k=1}^{p}[\mathbf{X}_0(i,j,k)-\bar{\mathbf{X}}_0][\mathbf{X}_1(i+\alpha,j+\beta,k+\gamma)-\bar{\mathbf{X}}_1]}{\sqrt{\sum_{i=1}^{m}\sum_{j=1}^{n}\sum_{k=1}^{p}[\mathbf{X}_0(i,j,k)-\bar{\mathbf{X}}_0]^2\sum_{i=1}^{m}\sum_{j=1}^{n}\sum_{k=1}^{p}[\mathbf{X}_1(i+\alpha,j+\beta,k+\gamma)-\bar{\mathbf{X}}_1]^2}} \tag{8}$$

used to turn the result to special domain. To calculate the denominator part, the summed-area tables algorithm [15] was used to compute the image sum and image energy sum under the feature, and then the standard deviation of the feature can be computed. With this algorithm, the computation time is greatly saved. The FNCC improves the computational efficiency. The best matching region is $\rho = \rho_{\max}$. The difference of coordinate between the kernel region and the best matching region indicates the displacement of the needle, dividing the displacement by time, the speed of the needle is obtained. It is used as the second measurement of Kalman filter.

3 Simulations

Several simulations with Field II [16], [17] have been done. The parameters used in Field II are given in Table 1.

Table 1: Parameters used in Field II

Name of parameter	Value
Transducer center frequency [MHz]	7.5
Sampling frequency [MHz]	27
Speed of sound [m/s]	1540
Elements of the probe	128
Width of element [mm]	0.1
Height of element [mm]	10
Kerf [mm]	0.017
Focal depth [mm]	50
Range of scan lines [degree]	[-20 20]
Range of scan planes [degree]	[-20 20]

The simulations are done on a series of homogeneous phantom with a metal needle whose radius is 0.5 mm. The size of the phantom is $50\times50\times30$ mm^3. For the homogeneous background, the spatial distribution of scatters is uniform distribution, and the spatial density of scatters is 10/mm^3. The reflection coefficient is K distribution [18], with $\nu = 10$, $\lambda = \sqrt{\nu}$. For the metal needle, the spatial distribution of the scatters is uniform distribution with the spatial density of scatters 125/mm^3. The reflection coefficient is set to 7.5 as constant amplitude. In the 3D simulated US volume, there are 53 planes/volume, 71 lines/plane and 2608 samples/line. In the simulated US volume, the exact position of needle is known, so the error between the simulation results and the ground truth values is evaluated.

In the simulation of speckle tracking method, the size of kernel region is set to 7*21*51 (plane * beam * sample), and size of the searching region is 11*37*61.

The first simulation is to compare the root mean square error (RMSE) of the RANSAC and RANSAC and Kalman filter method in a static situation. RANSAC algorithm and RANSAC and Kalman filter were used to estimate the direction angle and the tip position of the electrode of the same length. 50 simulations were done in order to calculate the RMSE. The length of the electrode tested is from 5 mm to 20 mm.

Figure 2 shows the RMSE of the estimation results of the direction angles with different length. The RANSAC and Kalman filter method gives a much less RMSE than the RANSAC algorithm only, especially when the needle length is less than 11 mm. Figure 3 gives the RMSE of the estimation result of the x, y, z coordinate and the needle tip

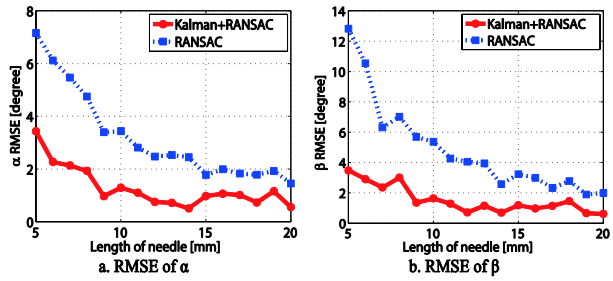

Figure 2: The RMSE of direction angles in a static situation. (Dotted square line: RANSAC; Solid point line: RANSAC + Kalman)

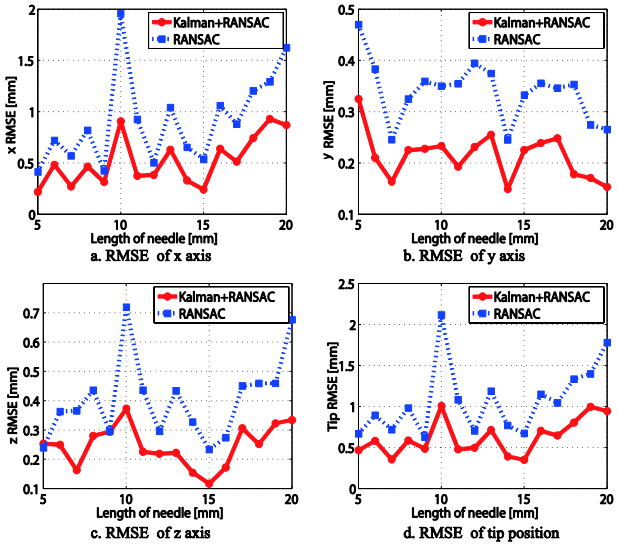

Figure 3: The RMSE of x, y, z coordinate and the RMSE of tip position in a static situation. (Dotted square line: RANSAC; Solid point line: RANSAC + Kalman)

with different length. It is obvious that the method RANSAC and Kalman can also reduce the RMSE of the tip position. The average percentage improved by RANSAC and Kalman filter method was given in Table 2. That is to say that for a constant position, the proposed method can give a more robust estimation of the position than RANSAC algorithm only.

The second simulation is to use RANSAC and Kalman filter to track a moving needle in a series of 16 simulated ultrasound volumes and estimate the position of metallic needle. The inserting speed is 1mm/s and the unit direction vector of the electrode is [0.94, 0, 0.34]. The initial length of the inserted needle is 5 mm. The aim of this experiment is to simulate a dynamical situation of the moving needle. For each simulation the estimation is performed 50 times.

Figure 4 and Figure 5 give the RMSE of the direction angles as well as the RMSE of x, y, z coordinate and tip position respectively. Because the Kalman filter needs initialization, for the first two volumes, the output result of RANSAC and Kalman is the same as that of RANSAC. The Kalman filter begins to work from the 3rd volume. From these two figures, it is obvious that the RMSE of RANSAC and Kalman is smaller than that of RANSAC only. The average percentage improved by RANSAC and Kalman was also shown in Table 2. So in the constant speed needle inserted situation, the proposed method also gives a more robust performance than RANSAC algorithm only.

Table 2: Average improvement thanks to RANSAC and Kalman method compared with RANSAC

	Static situation	Dynamic situation
α	58%	37%
β	68%	36%
X axis	40%	30%
Y axis	40%	24%
Z axis	36%	30%
Tip position	40%	30%

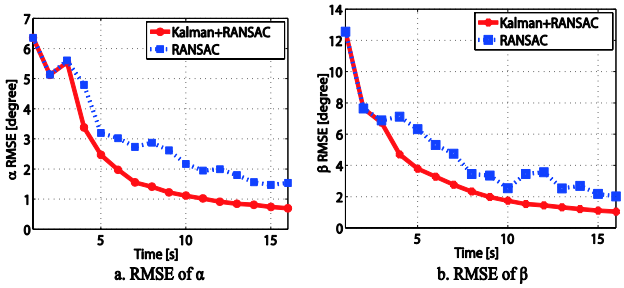

Figure 4: The RMSE of direction angles in a dynamic tracking situation. (Dotted square line: RANSAC; Solid point line: RANSAC + Kalman)

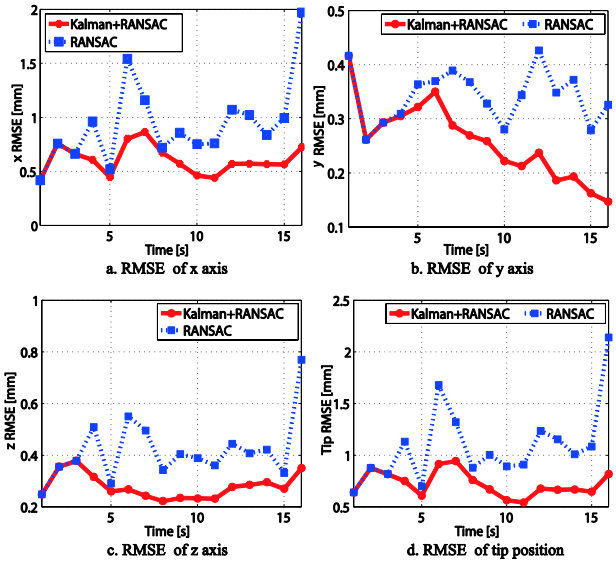

Figure 5: The RMSE of x, y, z coordinate and the RMSE of tip position in a dynamic tracking situation, the speed of insertion is 1 mm/s. (Dotted square line: RANSAC; Solid point line: RANSAC + Kalman)

4 Conclusion

RANSAC algorithm depends on randomly selected models, and sometimes there is a large error in the returned result. In order to avoid the large error which appears randomly, the Kalman filter is added. The simulations show that in either the constant situation or the dynamical situation, RANSAC and Kalman performs better than using RANSAC algorithm only. With Kalman filter, the tracking results are more stable, and the estimate error can also be reduced.

In further researches, the RANSAC and Kalman filter method will be tested on real data. To avoid the extreme noisy background in real data, the acquisition volume will be reduced by defining a region of interest (ROI), which contains the estimated position of the needle.

Acknowledgments

This work has been partially supported by the Centre Lyonnais d'Acoustique (CeLyA), ANR grant n°2011-LABX-014.

References

[1] M. A. Fischler and R. C. Bolles, “Random sample consensus: a paradigm for model fitting with applications to image analysis and automated cartography,” *Commun. ACM*, vol. 24, no. 6, pp. 381-395, 1981.

[2] B. Dong, E. Savitsky, and S. Osher, “A Novel Method for Enhanced Needle Localization Using Ultrasound-Guidance,” *Advances in Visual Computing*, pp. 914–923, 2009.

[3] S. Khosravi, R. Rohling, and P. Lawrence, “One-step Needle Pose Estimation for Ultrasound Guided Biopsies,” in *Engineering in Medicine and Biology Society, 2007. EMBS 2007. 29th Annual International Conference of the IEEE*, 2007, pp. 3343–3346.

[4] Z. Yaniv et al., “Needle-based interventions with the image-guided surgery toolkit (IGSTK): from phantoms to clinical trials.,” *IEEE transactions on bio-medical engineering*, vol. 57, no. 4, pp. 922-933, Apr. 2010.

[5] J. Stoll and P. Dupont, “Passive markers for ultrasound tracking of surgical instruments,” *Medical Image Computing and Computer-Assisted Intervention–MICCAI 2005*, pp. 41–48, 2005.

[6] M. Barva, M. Uhercik, J. Mari, and J. Kybic, “Parallel integral projection transform for straight electrode localization in 3-D ultrasound images,” *IEEE Transaction on Ultrasounics, Ferroelectrics, and Frequency Control (UFFC)*, vol. 55, no. 7, pp. 1559-1569, 2008.

[7] M. Uhercik, J. Kybic, H. Liebgott, and C. Cachard, “Model fitting using RANSAC for surgical tool localization in 3D ultrasound images,” *Biomedical Engineering, IEEE Transactions on*, vol. 57, no. 8, pp. 1907–1916, 2010.

[8] F. Gaufillet, H. Liegbott, M. Uhercik, F. Cervenansky, J. Kybic, and C. Cachard, “3D Ultrasound real-time monitoring of surgical tools,” in *Ultrasonics Symposium (IUS), 2010 IEEE*, 2010, pp. 2360–2363.

[9] R. E. Kalman, “A new approach to linear filtering and prediction problems,” *Transactions of the ASME--Journal of Basic Engineering*, vol. 82, no. Series D, pp. 35-45, 1960.

[10] G. Welch and G. Bishop, “An Introduction to the Kalman Filter,” no. UNC-Chapel Hill, TR 95-041, 2006.

[11] E. Building, “Speckle tracking for multi-dimensional flow estimation,” *Ultrasonics*, vol. 38, pp. 369-375, 2000.

[12] D. E. Robinson, F. Chen, and L. S. Wilson, “Measurement of velocity of propagation from ultrasonic pulse-echo data,” *Ultrasound in medicine biology*, vol. 8, no. 4, pp. 413-420, 1982.

[13] G. E. Trahey, J. W. Allison, and O. T. Von Ramm, “Angle independent ultrasonic detection of blood flow.,” *IEEE Transactions on Biomedical Engineering*, vol. 34, no. 12, pp. 965-967, 1987.

[14] J. P. Lewis, “Fast normalized cross-correlation,” in *Vision Interface*, 1995, vol. 10, no. 1, pp. 120-123.

[15] F. Crow, “Summed area tables for texture mapping,” *Computer Graphics SIGGRAPH proceedings*, vol. 11, no. 3, pp. 200-220, 1984.

[16] J. Jensen, “Field: A program for simulating ultrasound systems,” *CONFERENCE ON BIOMEDICAL IMAGING, VOL. 4,*, vol. 34, pp. 351- 353, 1996.

[17] J. a Jensen and N. B. Svendsen, “Calculation of pressure fields from arbitrarily shaped, apodized, and excited ultrasound transducers.,” *IEEE transactions on ultrasonics, ferroelectrics, and frequency control*, vol. 39, no. 2, pp. 262-267, Jan. 1992.

[18] H. Liebgott, O. Bernard, C. Cachard, and D. Friboulet, “Field simulation parameters design for realistic statistical parameters of Radio-Frequency ultrasound images,” in *IEEE International Ultrasonics Symposium*, 2007, pp. 2247-2250.